

Effect of Extreme ENSO and IOD on the Variability of Chlorophyll-a and Sea Surface Temperature in the North and South of Central Java Province

Kunarso^{1*}, Dwi Haryo Ismunarti¹, Aziz Rifa'i¹, Bayu Munandar¹, Anindya Wirasatriya¹,
R. Dwi Susanto^{1,2}

¹Department of Oceanography, Faculty of Fisheries and Marine Science, Universitas Diponegoro
Jl. Jacob Rais, Tembalang, Semarang 50275 Indonesia

²Department of Atmospheric and Oceanic Science, University of Maryland
College Park, MD 20742, USA
Email: kunarsojpr@yahoo.com

Abstract

Chlorophyll-a (chl-a) and Sea Surface Temperature (SST) are important indicators of air-sea interaction and primary productivity. It has been widely known that the variability of chl-a and SST in the waters of Central Java Province (CJP) is influenced by the monsoonal cycle. Previous studies did not clearly describe the variability of chl-a and SST when compared to other cycles. This present study investigated the variability of chl-a and SST influenced by monsoonal cycles, IOD, and ENSO in both CJP waters. Our analysis is based on satellite observations and uses daily data to compile climatological data. The analysis found differences between the variability of chl-a and SST during the monsoonal cycle and ENSO-IOD extreme conditions. During the monsoonal cycle, the maximum (minimum) chl-a (SST) in northern CJP is 0.7 mg.L⁻¹ (28.5°C) is observed in the West Monsoon, and in the southern CJP is 1.5 mg.L⁻¹ (25.5°C) is observed in the East Monsoon. In addition, the analysis reveals that the ENSO and IOD extremes do not clearly alter the variability of chl-a and SST in the northern CJP. However, ENSO and IOD extremes have clearly altered the variability of chl-a and SST in the southern CJP. The highest impact to variability of chl-a and SST occurred during IOD+ extreme (2019), where the range of value chl-a (SST) in south CJP is 0,35–4,57 mg.L⁻¹ (23,29 – 30,49°C). The value of chl-a (SST) is greater than 4 mg.L⁻¹ (less than 24°C) are observed in the east monsoon. It is caused by the intensity of lifting the mass of water from deeper waters to the sea surface, which possibly supplies the nutrients in the surface waters. The result of the investigation showed that the increasing of chl-a and decreasing of SST in the northern CJP dominant by monsoonal cycle and southern CJP dominant by monsoonal cycle and ENSO – IOD.

Keywords: Chlorophyll-a, SST, ENSO, IOD, Central Java

Introduction

Chlorophyll-a (chl-a) and Sea Surface Temperature (SST) are important indicators of air-sea interactions (Wirasatriya et al., 2019; Setiawan et al., 2019; Kunarso et al., 2020). Previous studies have found that the variability of chl-a and SST in the surface ocean is defined by upwelling, run-off from the mainland, vertical mixing, etc (Wang and Tang, 2014; Kim et al., 2014; Kunarso et al., 2018). Upwelling and vertical mixing can trigger the lifting of water masses from deeper waters and land runoff can be a distribution of water masses from land to estuaries. This process has a very important role in the variability of chl-a and SST at the surface ocean. The above mechanism has the same pattern, where the mechanism is a bridge to supply water masses that are rich in nutrients and makes the value of chl-

a (SST) increase (decrease). Primary mechanisms for high or low of chl-a and SST in Java Sea (JS) and Indonesian Ocean (IO) are upwelling, run-off from the mainland, and vertical mixing (Wang and Tang, 2014; Kim et al., 2014). Thus, this mechanism can provide nutrients for the growth of phytoplankton and affect the high/low SST.

The CJP has two different waters, JS in the north and IO in the south, centered on the regions of 109°–111.5° E and 5°–10° S. These both waters are home of the ten largest fisheries in Indonesia (BPS-Statistics Indonesia, 2020). Both waters in the CJP have complex air-sea and hydrodynamic interactions (Kao and Yu., 2009; Lan et al., 2019; Wirasatriya et al., 2020). The generally parallel coastline in CJP has a water depth that ranges from 0

to 60 m (north water) and 0–2000 m (south water) (Figure 1.).

Monsoon wind affects marine ecosystems and oceanographic conditions in both JS and IO. West (East) Monsoon blows during DJF (JJA) to bring warm (cold) air province (Wirasatriya *et al.*, 2020). The West and East Monsoons increased chl-a and lowered SST in the Indonesian Seas through the water mixing process (Zhang *et al.*, 2014; Vic *et al.*, 2019; Munandar *et al.*, 2021), upwelling (Setiawan and Habibi, 2011; Wirasatriya *et al.*, 2021; Susanto *et al.*, 2001), run-off from the mainland (Kim *et al.*, 2014), and latent heat release (Atmadipoera *et al.*, 2018; Wirasatriya *et al.*, 2019).

The effect of monsoon winds on the variability of chl-a and SST in Indonesian waters, related to ENSO and IOD variability. Predictions of the effect of ENSO and IOD on chl-a and SST in the Java Sea or Indonesian Ocean have been carried out, for example by Susanto *et al.* (2001), Wirasatriya *et al.* (2017), Setyohadi *et al.* (2021). None of them extend their observations by comparing the waters of the Java Sea

and Indian Ocean. Despite both seas having similar wind conditions that cause variability of chl-a and SST (Purwanto *et al.*, 2021). However, both seas did not have the same pattern of variability in chl-a and SST. The objective of this study is to investigate the mechanisms responsible for these differences.

Materials and Methods

Analysis of variability of chl-a and SST in both seas in Central Java Province used high spatial and temporal resolution data from satellites. Chl-a data obtained from the Ocean-Colour Climate Change Initiative (OC-CCI) level 3, *i.e.*, daily and 0.04°x0.04° (Sathyendranath *et al.*, 2019; Munandar *et al.*, 2021). Then, SST data obtained from the Group for High-Resolution Sea Surface Temperature (GHRSSST) OSTIA level 4, *i.e.*, daily and 0.05°x0.05° (Wirasatriya *et al.*, 2021). OC-CI and OSTIA products are the result of reanalysis of data from multiple satellite sensors and field data (Sathyendranath *et al.*, 2019; Wirasatriya *et al.*, 2021). The analysis period for chl-a and SST spans from January 2009 to December 2020.

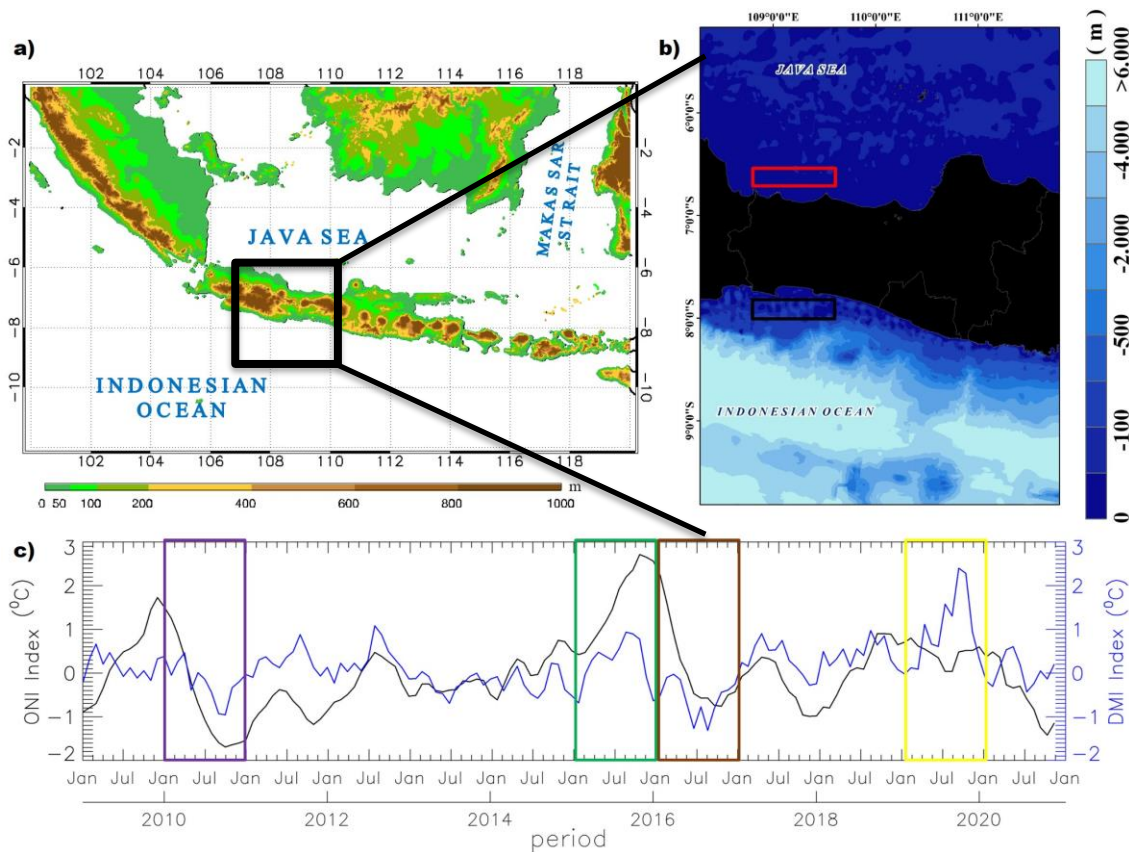


Figure 1. a). Map of the study area of interest, with detailed study region shown by the expended box, b): Topography and bathymetry condition in study area and its surroundings, c): Plotting time series of monthly ONI and DMI (La Nina Extreme (Purple Box); El Niño Extreme (Green Box); IOD- Extreme (Brown Box); IOD+ Extreme (Yellow Box)).

The cross-calibrated multi-platform (CCMP) data is used to understand the physical forcing's in the surface ocean. CCMP is level 3 data reanalysis and has a data spatial resolution of 0.25°x0.25° and a data recording interval of six hours. The accuracy of this wind product is higher than the other wind reanalysis data. All the analyses in the present study were sorted into monthly means, and then used to compile the monthly climatology by using the following equation:

$$\bar{X}(x,y) = \frac{1}{n} \sum_{i=1}^n xi(x,y,t)$$

Where is the monthly mean value or monthly climatology value at position (x, y), xi(x, y, t) is the *i*th value of the data at (x,y) position and time t. Furthermore, n is the number of data in 1 month and the number of monthly data in 1 period of climatology (i.e., from 2009 to 2020 = 11 data) for monthly calculation and monthly climatology calculation, respectively. If xi is not a number pixel, that pixel is excluded from the calculation.

Sea Level Anomaly (SLA) is reprocessed data from the Copernicus Marine Environment Monitoring Service (CMEMS). SLA data was obtained at level 4 with a spatial resolution of 0.25°x0.25°. Furthermore, the hourly precipitation product from ERA5 (reanalysis of ERA5 single levels) has a spatial resolution of 0.25°x0.25°. ERA5 is the fifth generation ECMWF reanalysis of the global climate and weather for the past 4 to 7 decades (Hersbach *et al.*, 2018). For the vertical profile of phosphate (PO4) concentrations from CMEMS with the spatial resolution of 0.25°x0.25° (Perruche, 2019). To describe the topography and bathymetry obtained from the Global 30 Arc-Second Elevation (GTOPO30) and General Bathymetric Chart of the Oceans (GEBCO). The phosphate data is used to investigate the vertical mass structure in both seas in central java province. Furthermore, to investigate other mechanisms of chl-a and SST variability in CJP waters, an analysis of El Niño Southern Oscillation (ENSO) and Indian Ocean Dipole (IOD) data was carried out. The Oceanic Niño Index (ONI) and Dipole Mode Index (DMI) are used to analyze ENSO and IOD. ONI obtained NINO 3.4 and DMI for the period January 2009–December 2020. To determine the relationship between variables, we performed regression analysis (Chicco *et al.*, 2021).

Result and Discussion

Seasonal variability of chl-a and SST

This research focuses on seasonal variability to determine the impact of ENSO and IOD on chl-a and SST in both seas in the CJP. The monthly climatology of chl-a, SST and wind speed provides an

overview of the variability of chl-a and SST in CJP (Figures 2 and 3.). The higher chl-a concentrations are typically observed during the WM season on north and south CJP during the EM (Figures 2 and 3.). The highest chl-a was in the northern CJP in January and in the southern CJP in August. Furthermore, reduced chl-a concentration occurs in March – May and September – November.

Figures 2(b) and 3(b) show the spatial distribution of the monthly climatology SST in both seas CJP, it is clear that a seasonal cycle occurs. Susanto *et al.* (2005); Wirasatriya *et al.* (2019) found that chl-a, SST and wind speed have good correlations in the Indonesian Sea.

During the WM and EM cycles, SST cooling in the northern CJP is not clearly visible. However, the highest SST drop was clearly seen in southern CJP in the EM cycle. The lowest SST (26°C) occurred in only a few regions in southern CJP and other regions are warmer. The lower SST is typically observed during the EM in the southern CJP.

Figures 2c) and 3c) describe the distribution of the climatology of wind speed in the northern and southern of the CJP on EM and WM. The both seas show that the wind direction in the north and south of CJP changes based on the monsoon cycle. The wind speed in the southern CJP (± 6 m.s⁻¹) is higher than the northern CPJ (± 3 m.s⁻¹) in the EM. Conversely, the highest wind speed in WM occurs in both CJP seas (± 3 m.s⁻¹). Thus, it was found that the variability of chl-a and SST in the north and south of the CJP was different, despite the monsoon cycle being the same.

The mechanism of variability of chl-a and SST in the southern CJP can be explained by analyzing wind speed. The extracted data (Figure 1b) was used to investigate the effect of wind speed on chl-a and SST in the north and south CJP. The relation between wind speed, chl-a and SST is clearly shown in Figure 4a. The direction of wind speed in EM is dominated by moving parallel to the coast. This direction can bring water masses away from the coast and trigger coastal upwelling. Previous studies in the Indonesian Ocean have found that the coastal upwelling phenomenon occurs during the east monsoon (Susanto *et al.*, 2001; Wirasatriya *et al.*, 2020; Setyohadi *et al.*, 2021). The lifting water mass can drive nutrient-rich from the deeper ocean to the euphotic zone.

Additionally, wind speed did not significantly affect the variability of chl-a in the northern CJP (*r*= 0.08). However, the impact of wind speed on SST was more pronounced compared to chl-a (*r*=0.5), but not greater than that of southern CJP (*r*=-0.84). The wind speed does not trigger an upwelling phenomenon in

this area. The concentration of chl-a in the northern CJP looks the same in January-December, but increases slightly in December-February (West Monsoon) (Figure 4a.). An increase in chl-a in the northern CJP coincides with an increase in precipitation in the CJP Area (Figure 4b.). CJP has

many large rivers that disemboque into the Java Sea and Indonesian Ocean. The precipitation that falls on the mainland will flow through rivers and end up in the sea. This mechanism allows the supply of nutrients from the mainland, which causes an increase in chlorophyll-a in the northern CJP (Kim *et al.*, 2014).

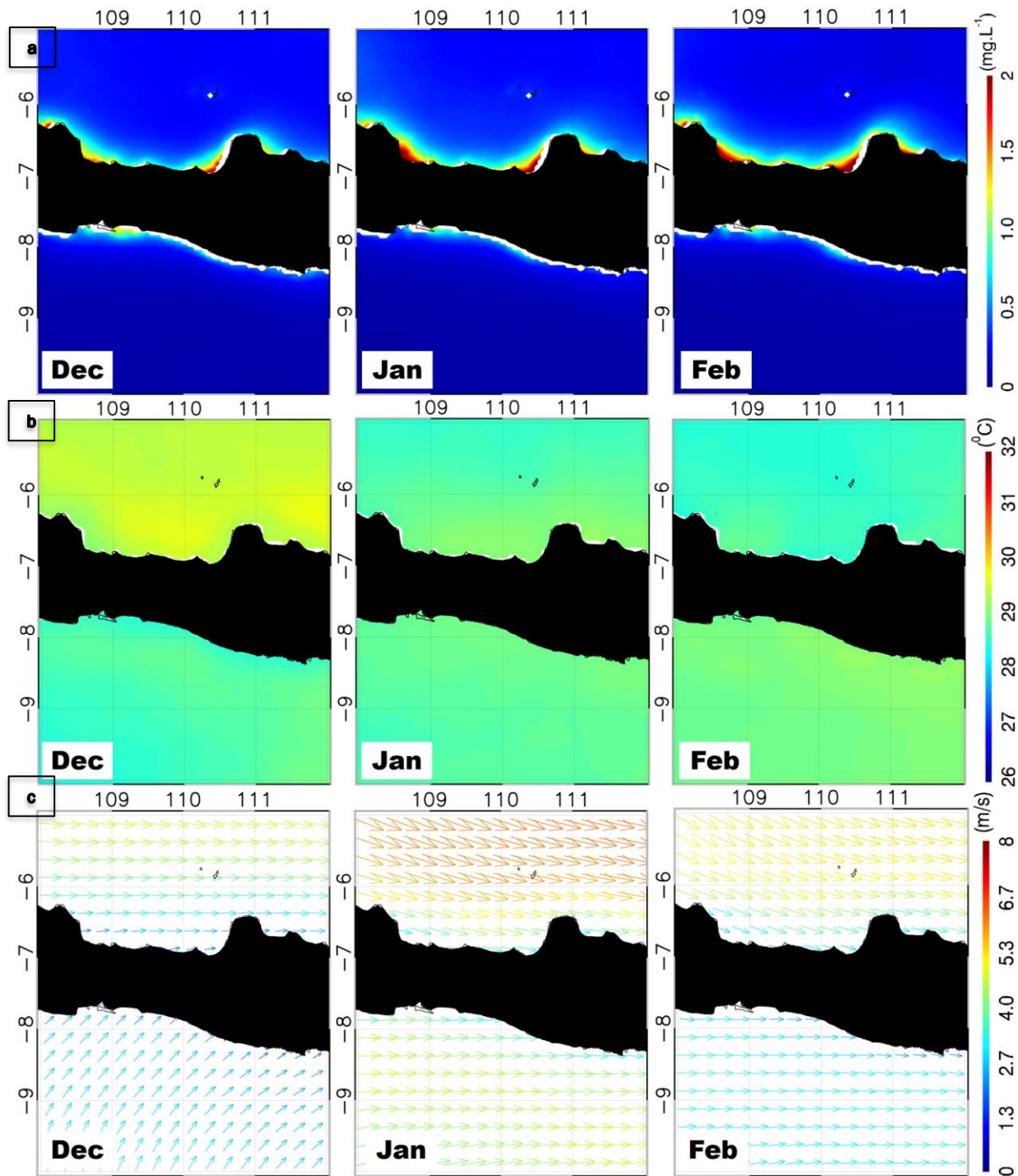


Figure 2. Monthly climatology of (a) chl-a, (b) SST, and (c) wind speed during the WM season.

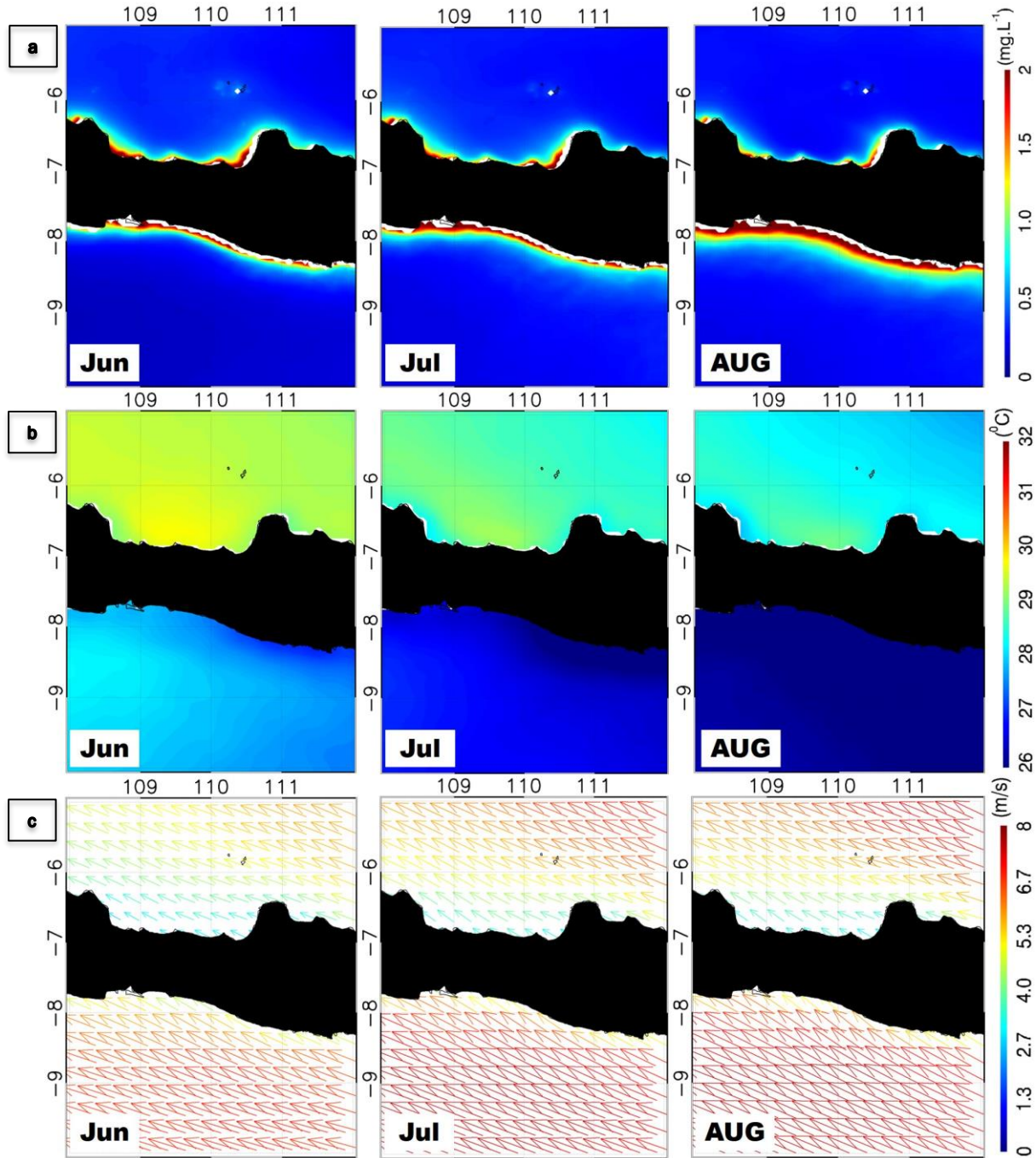


Figure 3. Monthly climatology of (a) chl-a, (b) SST, and (c) wind speed during the EM season.

The height concentration of chl-a in the northern and southern CJP is clearly shown to be influenced by nutrients from the deeper ocean to the euphotic zone. The pattern of chl-a concentrations in northern CJP increased in December and decreased in March. Furthermore, the chl-a concentration in southern CJP increased in May and decreased in November. Moreover, the height chl-a in the region vanishes during March–November (the northern CJP) and December – April (the southern CJP) (Figure 4a.).

The condition in northern CJP is likely due the wind speed does not trigger of upwelling phenomenon. Therefore, the supply of nutrients depends on the mainland run off. During the EM season, the intensity of precipitation in CJP has decreased ($<1 \text{ mm}\cdot\text{h}^{-1}$), so that the supply of nutrients from the mainland is reduced. Furthermore, the condition in southern CJP is likely due the wind speed being unfavorable for upwelling. During WM season, the southern CJP was dominated by low wind speed ($<4 \text{ m}\cdot\text{s}^{-1}$) and the

dominant wind direction was northwest to southeast, so upwelling did not occur. This hypothesis is in line with Wang and Tang (2014), who suggest that phytoplankton growth is controlled by the supply of nutrients to the euphotic zone.

Interannual variability of Chl-a and SST

To investigate the mechanism that controls the variability of chl-a and SST in the Indonesian Ocean, inter-annual cycles must be considered in addition to seasonal cycles (Wirasatriya *et al.*, 2017; Setiawan *et al.*, 2019). To obtain a comprehensive understanding of the mechanism controlling the variability of chl-a and SST, we also examined the effect of inter-annual cycles (ENSO and IOD). The analysis focuses on the highest and lowest ENSO and IOD in the last 12 years

(2009-2020) (Figure 1c.). The focus was investigated on the southern CJP because the variability anomalies of chl-a and SST were clearly delineated, whereas those in the northern CJP were not clearly delineated (Figure 5.). When ENSO and IOD reached their highest or lowest (extreme) values, the variability of chl-a and SST also experienced a large anomaly compared to monsoonal cycle conditions (Figure 6-9.). Especially in 2019, the southern CJP experienced the highest chl-a and the lowest SST when compared to other conditions. This large chl-a and SST anomaly are likely due to the high wind speed can trigger water mass lifting. The ENSO and IOD conditions were divided into four conditions (La Nina, El Niño, IOD- and IOD+), where La Nina and IOD- had lower chl-a and higher SST anomalous values when compared to El Niño and IOD+.

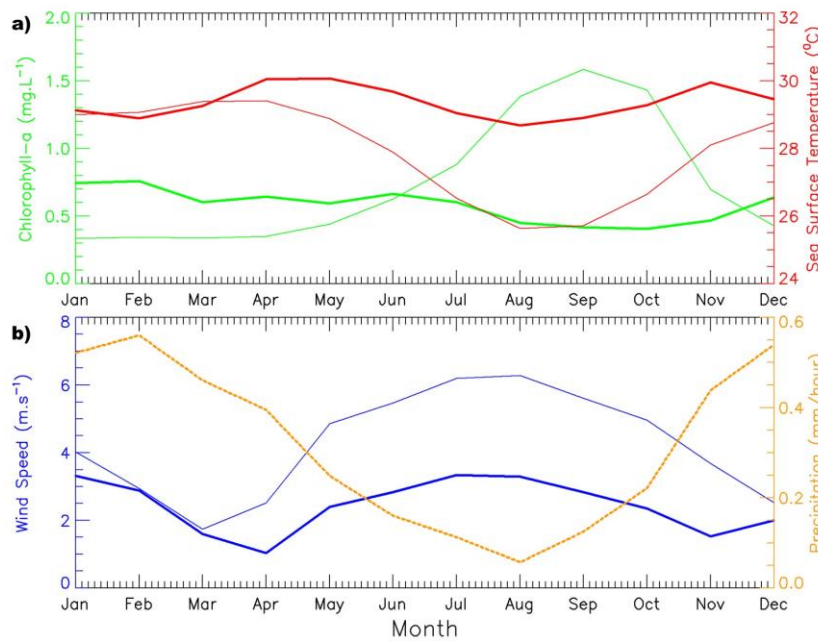


Figure 4. Plot time series of monthly climatology of (a) chl-a (green) and SST (red); (b) wind speed (blue) and precipitation (orange) in north (thick line) and south CJP (thin line).

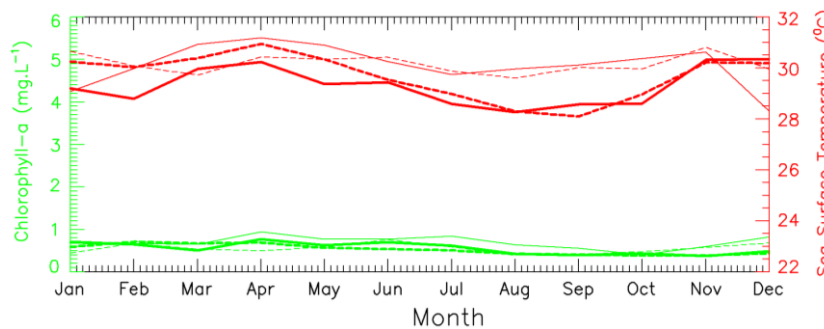


Figure 5. Plot time series of monthly of chl-a (green) and SST (red) when ENSO and IOD Extreme (La Nina Extreme (Thin Line); El Niño Extreme (Thick Line); IOD- Extreme (Thin Dot); IOD+ (Thick Dot)) in northern CJP.

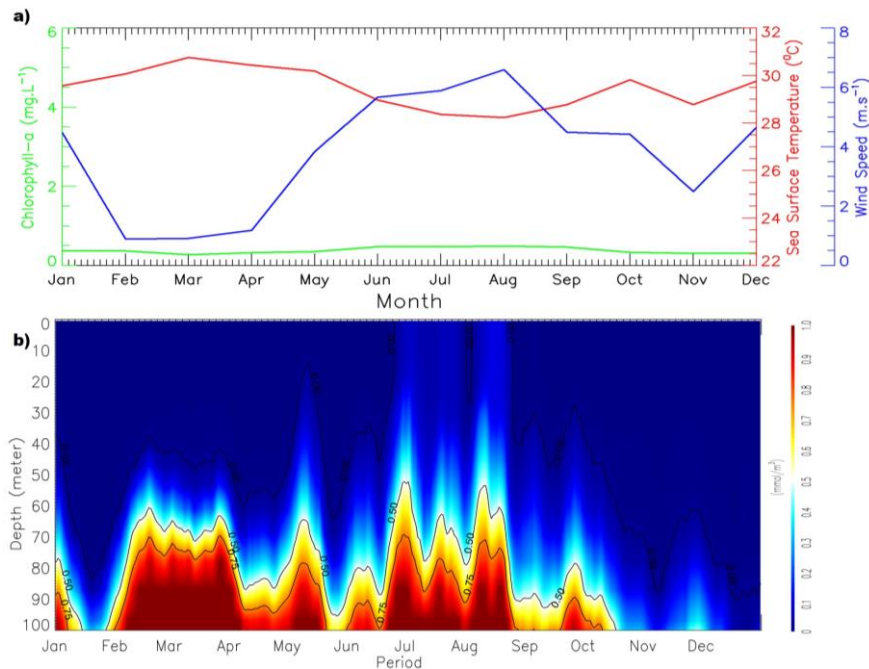


Figure 6. a). Plot time series of monthly of chl-a (green), SST (red), and wind speed (blue) when La Nina extreme (2010) events in south CJP, b). Profile vertical of phosphate south CJP.

During the occurrence of extreme La Nina and IOD- events (2010 and 2016), the variability anomaly of chl-a and wind speed decreased while SST increased comparison to the climatological value (Figures 6 and 7.). Figures 6a and 7a show that La Nina and IOD- events have the same effect on wind speed in southern CJP. The early termination of chl-a in 2010 and 2016 was affected by a lower wind speed over the southern CJP. The lower wind speed in La Nina and IOD- make the upwelling mechanism in the southern CJP unable to be generated. This is evidenced by the vertical profile of phosphate that does not lifting to the surface during La Nina and IOD- events (Figures 6b and 7b.). The absence of these mechanisms makes the supply of nutrients and cold temperatures from the deeper sea reduced. This deficiency makes the values of chl-a and SST during La Nina and IOD- events lower and more warm than the climatological values.

When the extreme El Niño event occurred in 2015, the variability of chl-a and wind speed increased and SST decrease. It was the opposite in sign compared to extreme La Nina and IOD- events. The highest increases in chl-a, wind speed and decreased of SST experienced differences in the time of occurrence. where the wind speed increased first (starting in April), but chl-a and SST were clearly seen in July (Figure 8a.). This time (April-September) difference is probably due to the waiting time in the lifting of the water mass from the deeper sea to the surface. This waiting time can be seen from the lifting

of the phosphate concentration which starts in April (80 meters) and reaches its peak in September (surface). The highest concentration of phosphate brought from the deeper sea was seen to be the same as the highest concentration of chl-a and the lowest SST (September). This proves that the upwelling mechanism in the southern CJP greatly affects the variability of chl-a and SST in that region.

Moreover, the interesting thing that was found was the effect of IOD+ on the variability of chl-a, SST and wind speed in southern CJP. During extreme IOD+ events that occurred in 2019, chl-a concentrations and wind speed increased and SST decrease significantly. This increase and decrease in value is 2-4 times greater than the climatological, La Nina, IOD- and El Niño values (Figure 9a.). The mechanism that causes the phenomenon is upwelling, but the upwelling in 2019 looks bigger than in 2015 (as seen from the vertical phosphate profile) (Figures 8b and 9b.). Previous research (Safinatunnajah *et al.*, 2021) found that in 2019, there was a Kelvin wave moving from the Africa waters to the south of the CJP. Kelvin waves reaching south of the CJP cause an increase in the intensity of upwelling in the area, which is indicated by a decrease in sea level.

In order to investigate further whether there is really a decrease in sea level in the south of Java, an analysis of the Sea Level Anomaly (SLA) value was carried out. The result shows that the sea level at the time of extreme IOD+ events is lower than the

extreme events of La Nina, IOD- and El Niño (Figure 10.). This implies that IOD+ plays a major role in increasing the chl-a concentration and lower SST in southern CJP compared to La Nina, El Niño or IOD-. This is reinforced by the conditions in 2015, where in

addition to the El Niño extreme event in the same year, the IOD+ value also increased (Figure 1c.). This hypothesis is in line with Wirasatriya *et al.* (2020), which states that IOD plays a more major role in the variability of chl-a and SST than ENSO in the southern CJP.

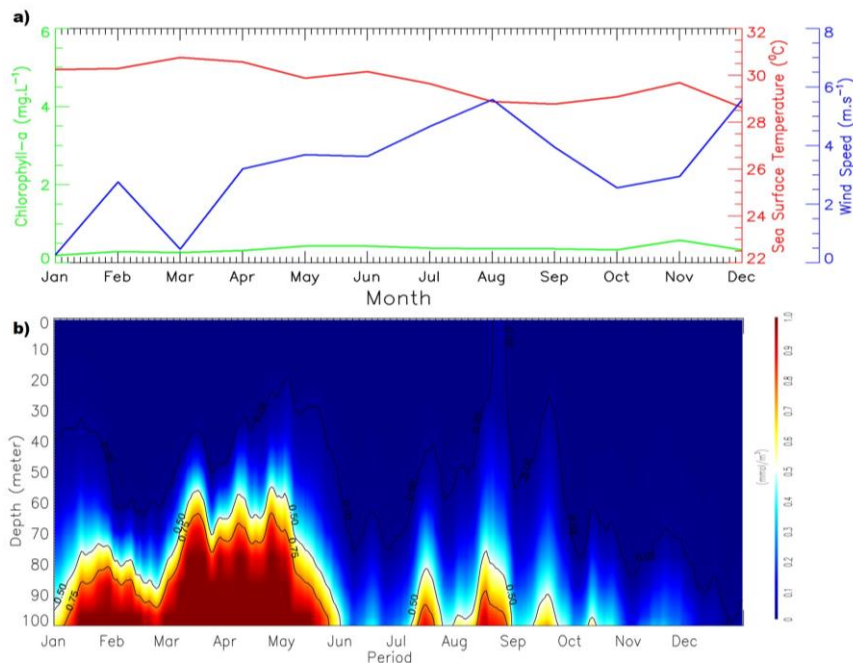


Figure 7. a). Plot time series of monthly of chl-a (green), SST (red), and wind speed (blue) when IOD- extreme (2016) events in south CJP, b). Profile vertical of phosphate south CJP.

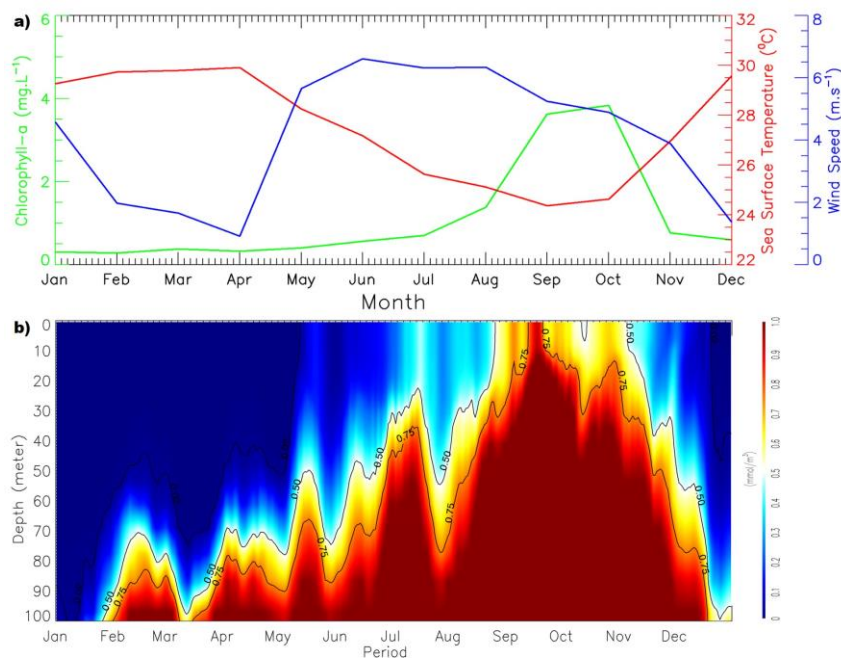


Figure 8. a). Plot time series of monthly of chl-a (green), SST (red), and wind speed (blue) when El Niño extreme events in south CJP, b). Profile vertical of phosphate south CJP.

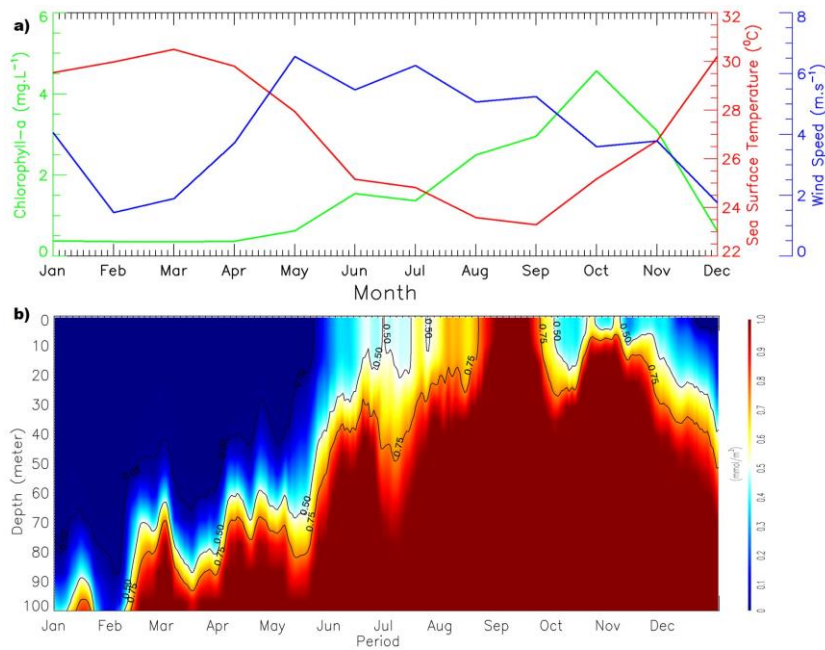


Figure 9. a). Plot time series of monthly of chl-a (green), SST (red), and wind speed (blue) when IOD+ extreme events in south CJP, b). Profile vertical of phosphate south CJP.

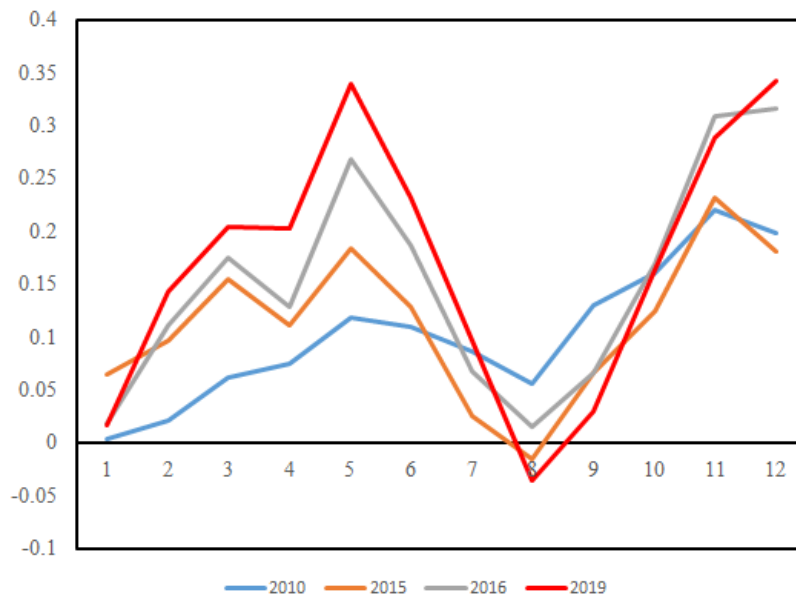


Figure 10. The value of sea level anomaly in the south of CJP under conditions of La Nina (Blue; 2010), El Nino (Orange; 2015, IOD- (Grey; 2016) and IOD+ (Red; 2019).

Conclusion

The results show that seasonal and interannual cycles of chl-a, SST and wind speed can be analyzed using time series data from satellite imagery. During the monsoon cycle, the variability of chl-a and SST in the northern CJP is dominantly

influenced by precipitation and the upwelling effect is clearly more dominant in the southern CJP. The values of increasing chl-a and decreasing SST in the northern and southern of CJP are inversely proportional, with December-February (WM) in the northern and July-October (EM) in the southern. Furthermore, during the interannual cycle the values of chl-a, SST and wind speed differences are clearly

illustrated. The lowest values of chl-a, and high SST occurred in La Nina and IOD- extreme events. Furthermore, the highest values of chl-a and lowest SST occurred during IOD+ events.

Acknowledgement

This study was financially supported by Faculty of Fisheries and Marine Sciences, Diponegoro University with contract number 58/UN7.5.10.2/PP/2021. R. Dwi Susanto thank to Adjunct Professor Program, World Class University, Universitas Diponegoro. GHRSSST Lv. 4 is provided by https://resources.marine.copernicus.eu/product-download/SST_GLO_SST_L4_REP_OBSERVATI-ONS_010_011 Meanwhile, OC-CCI data can be downloaded from <https://esa-oceancolour-cci.org/>. SLA and vertical profile of phosphate are from https://resources.marine.copernicus.eu/?option=com_csw&task=results. ONI index was obtained from <https://www.cpc.ncep.noaa.gov/data/indices/oni.ascii.txt>. Meanwhile the weekly DMI index is provided by <https://stateoftheocean.osmc.noaa.gov/sur/ind/dmi.php>. Thanks to RAK for contribution in this article.

References

- Atmadipoera, Khairunnisa, A.S.Z. & Kusuma, D.W. 2018. Upwelling characteristics during El Nino 2015 in Maluku Sea. *IOP Conf. Ser.: Earth Environ. Sci.*, 176(1): p.012018.
- BPS-Statistics Indonesia, 2020. Statistics of Capture Fishery Production 2000-2020. (Accessed 25 July 2022). <https://www.bps.go.id/statistable/2009/10/05/1705/produksi-perikanan-tang-kap-menurut-provinsi-dan-jenis-penangkapan-2000-2020.html>
- Chicco, D., Warrens, M.J. & Jurman, G. 2021. The coefficient of determination R-squared is more informative than SMAPE, MAE, MAPE, MSE and RMSE in regression analysis evaluation. *PeerJ Comput. Sci.*, 7: 1-24. <https://doi.org/10.7717/peerj-cs.623>.
- Hersbach, H., Bell, B., Berrisford, P., Biavati, G. & Horányi, A, 2018: ERA5 hourly data on single levels from 1959 to present. Copernicus Climate Change Service (C3S) Climate Data Store (CDS).
- Kao, H.Y. & Yu, J.Y. 2009. Contrasting eastern-Pacific and central-Pacific types of ENSO. *J. Clim.* 22: 615-632. <https://doi.org/10.1175/2008JCLI2309.1>.
- Kim, T., Najjar, R.G. & Lee, K. 2014. Influence of Precipitation Events on Phytoplankton Biomass in Coastal Waters of the Eastern United States. *Global Biogeochem. Cycles*, 28(1): 1-13. <https://doi.org/10.1002/2013GB004712>.
- Kunarso, Ismanto, A., Situmorang, R.P. & Wulandari, S. Y. 2018. Variability of Upwelling in Bone Bay and Flores Sea. *Int. J. Civ. Eng.*, 9(10): 742-751.
- Kunarso, Hadi, S., Ningsih, N.S., Baskoro, M., Wirasatriya, A. & Kuswardani, A.R.T.D. 2020. The classification of upwelling indicators base on sea surface temperature, chlorophyll-a and upwelling index, the case study in Southern Java to Timor Waters. *IOP Conf. Ser.: Earth Environ. Sci.*, 530(1): p.012020. <https://doi.org/10.1088/1755-1315/530/1/012020>.
- Lan, K.W., Chang, Y.J. & Wu, Y.L. 2019. Influence of oceanographic and climatic variability on the catch rate of yellowfin tuna (*Thunnus albacares*) cohorts in the Indian Ocean. *Deep Sea Res. Part II Top. Stud. Oceanogr.*, 175: p.104681. <https://doi.org/10.1016/j.dsr2.2019.104681>.
- Munandar, B., Wirasatriya, A., Sugianto, D.N., Ambariyanto & Sunaryo. 2021. Response of Wind Speed on Chlorophyll-a Variability in the Philippine Sea and North Maluku Sea. *Buletin Oseanografi Marina*. 10(3): 269-276. <https://doi.org/10.14710/buloma.v10i3.38273>
- Perruche, C., 2019. Product User Manual for the Global Ocean Biogeochemistry Hindcast Global_reanalysis_bio_001_029. Copernicus Marine Environment Monitoring Service.
- Purwanto, Sugianto, D.N., Zainuri, M., Permatasari, G., Atmodjo, W., Rochaddi, B., Ismanto, A., Wetchayont, P. & Wirasatriya, A. 2021. Seasonal Variability of Waves Within the Indonesian Seas and Its Relation With the Monsoon Wind. *ILMU KELAUTAN: Indonesian Journal of Marine Sciences*. 26(3): 189-196. <https://doi.org/10.14710/ik.ijms.26.3.189-196>.
- Safinatunnajah, N., Wirasatriya, A., Rifai, A., Setiyono, H., Ismanto, A., Setiawan, J.D. & Nugraha, A.L. 2021. Influence of 2019 strong positive IOD on the upwelling variability along the southern coast of Java. *IOP Conf. Ser.: Earth Environ. Sci.*, 919(1): p.012027. <https://doi.org/10.1088/1755-1315/919/1/012027>.
- Sathyendranath, S., Brewin, R. J., Brockmann, C., Brotas, V., Calton, B., Chuprin, A., Cipollini, P., Couto, A.B., Dingle, J., Doerffer, R. & Donlon, C. 2019. An Ocean-Colour Time Series for Use in Climate Studies: The Experience of the Ocean-Colour Climate Change Initiative (OC-CCI).

- Sensors 19(19): p.4285. <https://doi.org/10.3390/s19194285>.
- Setiawan, R.Y. & Habibi, A. 2011. Satellite Detection of Summer Chlorophyll-a Bloom in the Gulf of Tomini. *IEEE J. Sel. Top. Appl. Earth Obs. Remote Sens.*, 4(4): 944-948. <https://doi.org/10.1109/JSTARS.2011.2163926>.
- Setiawan, R.Y., Wirasatriya, A., Hernawan, U., Leung, S. & Iskandar, I., 2019. Spatio-Temporal Variability of Surface Chlorophyll-a in the Halmahera Sea and its Relation to ENSO and the Indian Ocean Dipole. *Int. J. Remote Sens.*, 41(1): 284-299. <https://doi.org/10.1080/01431161.2019.1641244>.
- Setyohadi, D., Zakiyah, U., Sambah, A. B. & Wijaya, A. 2021. Upwelling impact on sardinella lemuru during the indian ocean dipole in the bali strait, Indonesia. *Fishes*. 6(1): p.8. <https://doi.org/10.3390/fishes6010008>.
- Susanto, R.D., Gordon, A.L. & Zheng, Q. 2001. Upwelling along the coasts of Java and Sumatra and its relation to ENSO. *Geophys. Res. Lett.*, 28(8): 1599-1602. <https://doi.org/10.1029/2000GL011844>.
- Susanto, R. D., Moore, T. S. & Marra, J. 2005. Ocean color variability in the Indonesian Seas during the SeaWiFS era. *Geochem. Geophys. Geosyst.*, 7: p.Q05021. <https://doi.org/10.1029/2005GC001009>.
- Vic, C., Garabato, A.C.N., Green, J.A.M., Waterhouse, A.F., Zhao, Z., Melet, A., Lavergne, C.D., Buijsman, M.C. & Stephenson, G.R. 2019. Deep-ocean Mixing Driven by Small-scale Internal Tides. *Nat. Commun.*, 10(1): p.2099. <https://doi.org/10.1038/s41467-019-10149-5>.
- Wang, J.J. & Tang, D.L. 2014. Phytoplankton Patchiness during Spring Intermonsoon in Western Coast of South China Sea. *Deep Sea Res. Part II Top. Stud. Oceanogr.*, 101: 120-128. <https://doi.org/10.1016/j.dsr2.2013.09.020>.
- Wirasatriya, A., Prasetyawan, I.B., Triyono, C.D., Muslim & Maslukah, L. 2017. Effect of ENSO on the variability of SST and Chlorophyll-a in Java Sea. *IOP Conf. Ser.: Earth Environ. Sci.*, 116(1): 012063. <https://doi.org/10.1088/1755-1315/116/1/012063>.
- Wirasatriya, A., Sugianto, D.N., Helmi, M., Setiawan, R.Y. & Koch, M., 2019. Distinct Characteristics of SST Variabilities in the Sulawesi Sea and the Northern Part of the Maluku Sea During the Southeast Monsoon. *IEEE J. Sel. Top. Appl. Earth Obs. Remote Sens.*, 12(6): 1763-1770. <https://doi.org/10.1109/JSTARS.2019.2913739>.
- Wirasatriya, A., Setiawan, J.D., Sugianto, D.N., Rosyadi, I.A., Haryadi, Winarso, G., Setiawan, R.Y. & Susanto, R.D. 2020. Ekman Dynamics Variability along the Southern Coast of Java Revealed by Satellite Data. *Int. J. Remote Sens.*, 41(21): 8475-8496. <https://doi.org/10.1080/01431161.2020.1797215>.
- Wirasatriya, A., Susanto, R. D., Kunarso, Jalil, A. R., Ramdani, F. & Puryajati, A. D., 2021. Northwest Monsoon Upwelling within the Indonesian Seas. *Int. J. Remote Sens.*, 42(14): 5433-5454.
- Zhang, S., Xie, L., Hou, Y., Zhao, H., Qi, Y. & Yi, X., 2014. Tropical Storm-induced Turbulent Mixing and Chlorophyll-a Enhancement in the Continental Shelf Southeast of Hainan Island. *J. Mar. Sys.*, 129: 405-414. <https://doi.org/10.1016/j.jmarsys.2013.09.002>.